

## Influence of particle size on property of Ti–6Al–4V alloy prepared by high-velocity compaction

Zhi-qiao YAN<sup>1,2</sup>, Feng CHEN<sup>1</sup>, Yi-xiang CAI<sup>1</sup>, Jian YIN<sup>2</sup>

1. Department of Powder Metallurgy, Guangzhou Research Institute of Nonferrous Metals, Guangzhou 510650, China;

2. State Key Laboratory of Powder Metallurgy, Central South University, Changsha 410083, China

Received 10 November 2011; accepted 1 March 2012

**Abstract:** Three Ti–6Al–4V alloy powders with median diameters of 103, 66 and 44  $\mu\text{m}$ , respectively, were pressed by high-velocity compaction (HVC) technology and then sintered in vacuum. The effects of particle sizes on forming as well as properties of sintered samples were investigated. The results show that fine powders are more difficult to press than coarse powders and its compact density is lower too. But the sintered density of fine powders is obviously higher than that of coarse powders. Compared with the powders with 103 and 66  $\mu\text{m}$  in diameter, the green density with 44  $\mu\text{m}$  diameter powders is lower, which is 85.1% of theoretical density (TD) at an impact energy of 913 J. After sintering at 1300 °C for 2.5 h, the sintered density of the compacts with 44  $\mu\text{m}$  diameter powders is the highest, and reaches 98.2% of TD. Moreover, the sintered sample with 44  $\mu\text{m}$  in diameter has the highest hardness and compressive strength, which are HV 354 and 1265 MPa, respectively.

**Key words:** Ti–6Al–4V; high-velocity compaction (HVC); green density; sintering

### 1 Introduction

High-velocity compaction (HVC) was first discovered in 1960s [1]. In the past half century, various methods and equipments for compaction at a high velocity have been investigated. In recent decades, a renewed HVC technique was put forward, and has realized large-scale commercialization based on the successful construction of hydraulic impact compaction equipment, too [2,3]. The hammer speed of the HVC impact machine can be controlled in the range of 2–30 m/s to transfer the compaction energy to the powder [4,5]. The endurance limit of such HVC moulds has been verified to exceed a minimum of 100000 cycles in a full-scale compaction test [6].

Many kinds of powder materials were studied using the HVC technique: metals (Cu [7], Fe [8]), ceramics ( $\text{Al}_2\text{O}_3$  [9]) and polymers (UHMWPE [10]). Research on iron-based is especially successful and has been applied to producing gear wheel components with 7.7 g/cm<sup>3</sup> density [11] in mass scale, which is notably higher compared with those produced by warm compaction

(WC) with 7.3–7.4 g/cm<sup>3</sup> density usually. In contrast, research on forming powders with intrinsic high work hardening rate, such as titanium and molybdenum, is very scarce. Pure titanium and titanium–hydroxyapatite mixture formed by HVC with good effects have been reported [12–14]. This suggests that HVC is an especially competitive method for forming powders difficult to densify through conventional compaction. Unfortunately, no further research about titanium alloy powder formed by HVC has been published up to date.

Ti–6Al–4V alloy is one of the most important and widely used titanium alloys accounting for more than a half of all titanium sales [15]. The conventional densification of the alloy is usually carried out by expensive hot isostatic pressing (HIP) after cold isostatic pressing (CIP) and sintering. It is meaningful to develop a near-net-shape and short-process fabricating method. It seems that HVC is a new possible method worthy of trying due to its adiabatic characteristic during compaction. In this work, the forming feature of Ti–6Al–4V alloy powders pressed by HVC was investigated. The sintered behaviors of compacts and properties of the sintered samples were also studied.

**Foundation item:** Project (51004040) supported by the National Natural Science Foundation of China; Project (20110952K) supported by Open Research Fund of State Key Laboratory of Powder Metallurgy of Central South University, China

**Corresponding author:** Zhi-qiao YAN; Tel: +86-20-61086627; E-mail: [zhiquiaoyan@sina.com](mailto:zhiquiaoyan@sina.com)

DOI: 10.1016/S1003-6326(13)62470-X

## 2 Experimental

### 2.1 Materials

Three types of hydride/dehydride Ti–6Al–4V alloy powders (Hebei Wuyi Co., Ltd., China) with median diameters of 103, 66 and 44  $\mu\text{m}$ , respectively were used. Characteristics and SEM images of the powders are shown in Table 1 and Fig. 1, respectively. No any lubricant or binder was added into the powders.

**Table 1** Characteristics of three Ti–6Al–4V alloy powders

Median diameter/ $\mu\text{m}$	Apparent density/ ( $\text{g}\cdot\text{cm}^{-3}$ )	w(O)/%	w(N)/%	w(H)/%	Powder image
103	1.52	<0.25	<0.03	<0.03	Irregular
66	1.34	<0.35	<0.03	<0.03	Irregular
44	1.11	<0.45	<0.03	<0.03	Irregular

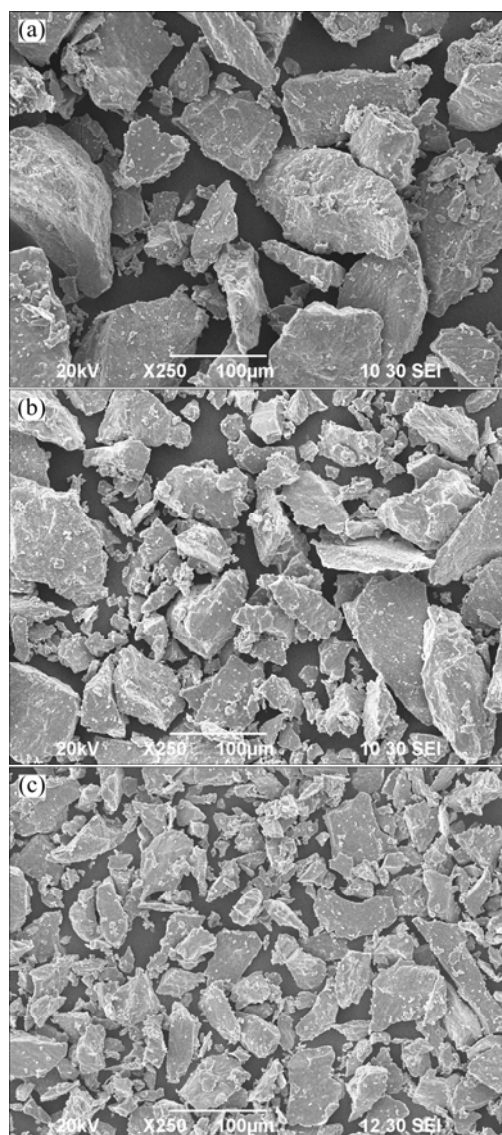


**Fig. 1** SEM images of three Ti–6Al–4V alloy powders with different diameters: (a) 103  $\mu\text{m}$ ; (b) 66  $\mu\text{m}$ ; (c) 44  $\mu\text{m}$

### 2.2 Equipment

The forming machine used was a HYP 35–7 typed HVC machine designed by Hydropulsor AB, Sweden. The equipment had a maximum impact energy of 7 kJ (approximately 350 t) per stroke and the hammer mass of 135 kg. The whole HVC process is made up of four steps, powder filling, pre-compacting, compacting and ejecting, similar to conventional compaction.

### 2.3 Specimen preparation

The powder was placed in a cylindrical die (inner diameter of 20 mm), which was situated in the above machine. Before powder filling, the die wall was lubricated with zinc stearate dissolved in acetone to facilitate the ejection of samples. For comparison, each powder filling height was fixed as 20 mm. Stroke length from 4 mm to 12 mm with 2 mm interval was adopted according to the size of samples and the withdraw force. Impact energy and velocity based on stroke length were calculated as 304–913 J and 2.12–3.68 m/s [12], respectively. Pressed samples were then sintered in a high vacuum ( $10^{-4}$  Pa) sintering furnace at 1300  $^{\circ}\text{C}$  for 2.5 h with a heating rate of 4  $^{\circ}\text{C}/\text{min}$ .

### 2.4 Test methods

The specimen density was determined by the Archimedes method, and relative density (RD) was calculated based on the theoretical density (TD) of 4.43  $\text{g}/\text{cm}^3$  for Ti–6Al–4V alloy. Polished sample cross-sections were etched with Kroll's reagent (3 mL HF+6 mL  $\text{HNO}_3$ +100 mL  $\text{H}_2\text{O}$ ) and observed with an optical microscope (OM). The hardness of specimen was characterized by the Vickers microhardness under a load of 19.6 N for 15 s. The compressive tests (cylindrical samples with 4 mm in diameter and 6 mm in height) were carried out with a universal testing machine at a speed of 0.5 mm/min. The load and displacement obtained through compressive tests were converted to true stress and true strain [15].

## 3 Results and discussion

### 3.1 Green density analysis

The green densities of three powders are presented in Fig. 2. It shows that the green density of powders with 103  $\mu\text{m}$  in diameter increases slowly with increasing impact energy, while that with 66 or 44  $\mu\text{m}$  in diameter increases faster, especially above the impact energy of 761 J. At the same impact energy, the green density of powder with 103  $\mu\text{m}$  in diameter is the highest and that with 44  $\mu\text{m}$  is the lowest, and the maximum density difference between them is 0.53  $\text{g}/\text{cm}^3$  at the lowest impact energy of 304 J. The difference decreases with increasing impact energy, and becomes 0.09  $\text{g}/\text{cm}^3$  only

at the impact energy of 913 J. In contrast, the green densities with 66 and 44  $\mu\text{m}$  in diameter of powders are close to each other, and the difference between them is in the range of 0.07–0.16  $\text{g}/\text{cm}^3$ . The maximum relative densities of compacts are 87.2%, 86.6% and 85.1% for powders with 103, 66 and 44  $\mu\text{m}$  in diameter, respectively. The density is slightly higher than that of green compact prepared by blending of powders and CIP process, which is approximately 85% TD [16].

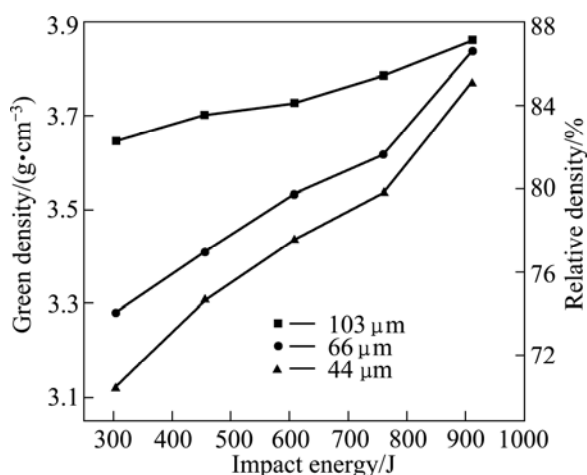


Fig. 2 Green and relative densities of three Ti-6Al-4V alloy powders with different diameters

As the impact energy increases, the energy absorbed by powder particles increases correspondingly according to the energy conservation law, which leads to increasing the green density continuously. When the impact energy is low, the densification of the powders is mainly in the form of sliding, filling pores and rearranging of powder particles. Powder with 103  $\mu\text{m}$  in diameter has the largest apparent density (Table 1), so it is easy to reach the highest green density due to its best filling ability. When the impact energy is above 761 J, a sudden increase of the green density for 66 and 44  $\mu\text{m}$  diameter powders occurs. It might be caused by sufficient displacement and rearrangement of particles. For the three powders, almost the same green density is obtained when the final impact energy is high enough. On the whole, the fine powder is more difficult to compress, and the effects of powder sizes on green density by HVC are similar to those by conventional compaction. However, lubricant or binder occupying a high volume fraction is usually necessary for titanium alloy powder formed through conventional compaction. It is concluded that HVC can press pure powder to higher density and is a clean method to prepare high performance titanium materials.

In our previous work about forming pure titanium powder by HVC technology, the maximum RD of compacts reaches 96.6% at the impact energy of 1217 J [12]. In the present work, the maximum impact energy

allowable in consideration of the withdraw force is only 913 J. Lower green density may be attributed to the deficiency of impact energy. It can be assumed that a higher green density could be realized under better lubricant condition and higher impact energy.

### 3.2 Sintered properties

Figure 3 shows the sintered density of green compacts. Compared with the curves of the green density, these curves exhibit an utterly converse change. The sintered density of 44  $\mu\text{m}$  diameter powder is the highest and that with 103  $\mu\text{m}$  in diameter is the lowest. The maximum sintered densities with 103 and 66  $\mu\text{m}$  in diameter are 4.08  $\text{g}/\text{cm}^3$  (92.1% RD) and 4.23  $\text{g}/\text{cm}^3$  (95.6% RD), respectively. Whereas the densities of all samples with 44  $\mu\text{m}$  diameter powder are in the range of 4.22–4.35  $\text{g}/\text{cm}^3$  (95.5%–98.2% RD). This is attributed to the better sintering activity of finer powders. Its beneficial effect on sintering surpasses the deficiency in compaction. The maximum sintered density of Ti-6Al-4V alloy prepared by HVC in this work is higher than that by metal injection moulding (MIM), and the relative densities are 96.0% [17] and 97.1% [18], respectively. For the green compact formed by CIP and sintered in vacuum, the densification degree usually reached 95% [16]. The sintered density by HVC is thus obviously competitive than MIM or CIP method. If blended elemental powders instead of alloy powders are used, the green density and sintered density might be improved further because of the better compressive ability and sintered activity of the elemental powder.

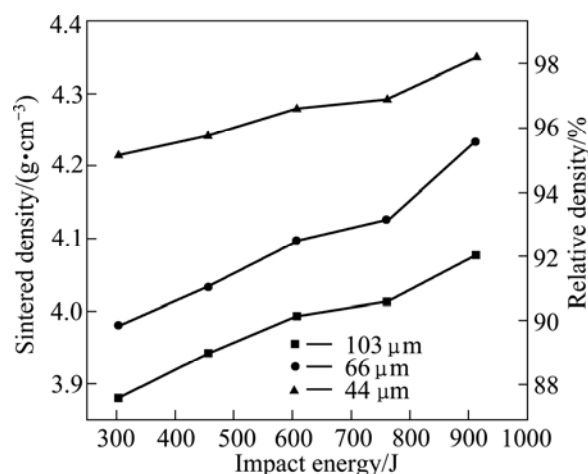
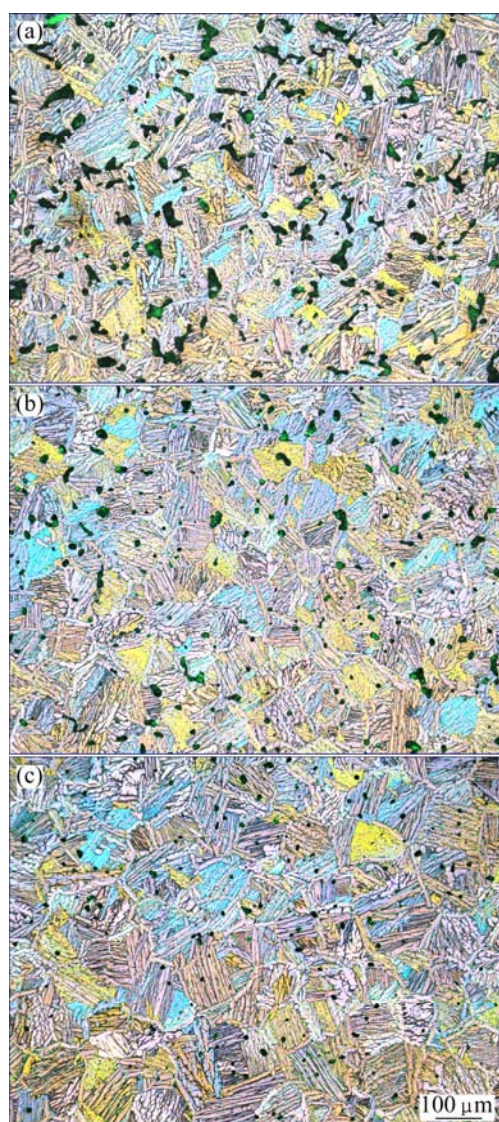


Fig. 3 Sintered density and relative density of three Ti-6Al-4V green compacts with different diameters

Figure 4 shows the optical micrographs of the three sintered alloy samples. They reveal a typical fully lamellar microstructure with the additional presence of pores. By comparing the features of the three samples, it can be found that with the refinement of powder particle

sizes, the grain size increases and the pores decrease. In the sample with 103  $\mu\text{m}$  diameter powder, the pores with irregular shape and some pore cluster regions (Fig. 4(a)) survive on the grain boundary. This indicates that an inadequate densification process occurs in the compact with 103  $\mu\text{m}$  diameter powder sintered at 1300  $^{\circ}\text{C}$ . While the pores become isolated and rounded (Fig. 4(b)) in the sample with 66  $\mu\text{m}$  diameter powder, which suggests that a relatively higher sintering densification happens. In contrast, only a few small and round pores (Fig. 4(c)) mainly survive in the grain of the sample with 44  $\mu\text{m}$  diameter powder, and the grain size is larger than that both in the samples with 66 and 44  $\mu\text{m}$  in diameter of powders. This means that this green compact could realize a sufficient densification through sintering process at 1300  $^{\circ}\text{C}$ . It also suggests that the heating rate of 4  $^{\circ}\text{C}/\text{min}$  seems too fast for 44  $\mu\text{m}$  diameter powder, so the grain grows severely and some pores exist in the grain.



**Fig. 4** Microstructures of three Ti-6Al-4V alloys with different diameters: (a) 103  $\mu\text{m}$ ; (b) 66  $\mu\text{m}$ ; (c) 44  $\mu\text{m}$

Hardness and compressive strength of three sintered samples with the maximum density were tested and the results are listed in Table 2. It is shown that hardness and compressive strength of powder sample with 44  $\mu\text{m}$  diameter is the highest, which are HV 354 and 1265 MPa, respectively. The hardness increases by 45.1% and compressive strength increases by 24.4% than those with 103  $\mu\text{m}$  diameter powder, respectively. And these are mainly attributed to the highest sintered density of sample with 44  $\mu\text{m}$  diameter powder.

**Table 2** Mechanical properties of three Ti-6Al-4V alloys

Median diameter/ $\mu\text{m}$	Relative density/%	Hardness, HV	Compressive strength/MPa
103	92.1	244	1017
66	95.6	301	1165
44	98.2	354	1265

Figure 5 shows the compression stress—strain curves of three sintered samples. These curves contain following three distinct regions, a linear elastic region, a long plateau stage with nearly constant flow stress to a large strain and a failure stage, where the flow stress decreases suddenly. When compressed, the alloy is elastically compressed up to about the proportional limit at first. And then the flow stress increases due to the strain hardening up to the maximum flow stress after the initial yielding. Finally, the flow stress starts to decrease and the fracture occurs. The decrement of flow stress with increasing strain is due to the effect of unstable deformation such as development of flow localization, microcracks. It can be assumed that pores have an important side effect on the compressive strength. A further work will focus on obtaining higher green density on the basis of better lubricant conditions and samples with large size will be fabricated to study the comprehensive mechanical properties.

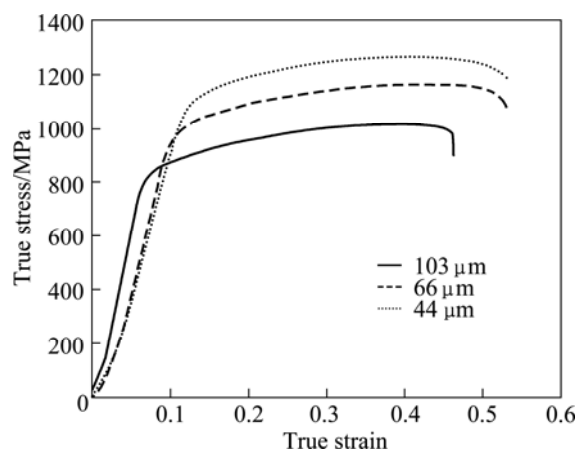


**Fig. 5** True stress—strain curves of three Ti-6Al-4V alloys with different diameters under compressive tests

## 4 Conclusions

1) Ti–6Al–4V alloy powder can be pressed into compact with a relatively high green density by HVC technology. The maximum green density reaches no less than relative density of 85% for different particle sizes.

2) With reducing particle sizes, the green density decreases, whereas the sintered density increases. By comparison, samples with 44  $\mu\text{m}$  diameter powder have the lowest green density (relative density of 85.1%) and the highest sintered density (relative density of 98.2%).

3) After sintering at 1300  $^{\circ}\text{C}$  for 2.5 h, the alloy powder with 44  $\mu\text{m}$  diameter has the highest hardness and compressive strength, which are HV 354 and 1265 MPa, respectively.

4) HVC technology provides a clean and new short process for preparing high performance titanium alloys.

## References

- [1] SETHI G, MYERS N S, GERMAN R M. An overview of dynamic compaction in powder metallurgy [J]. *Int Mater Rev*, 2008, 53(4): 219–224.
- [2] QU Xuan-hui, YIN Hai-qing. Development of powder high velocity compaction technology [J]. *Materials China*, 2010, 29(2): 45–49. (in Chinese)
- [3] DOREMUS P, GUENNEC Y L, IMBAULT D, PUENTE G. High-velocity compaction and conventional compaction of metallic powders; comparison of process parameters and green compact properties [J]. *Proc IMechE, Part E: J Process Mechanical Engineering*, 2010, 224 (3): 177–185.
- [4] SKOGLUND P. High density PM parts by high velocity compaction [J]. *Powder Metall*, 2001, 44(3): 199–201.
- [5] SKOGLUND P, KEJZELMAN M, HAUER I. HVC punches PM to new mass production limits [J]. *Met Powder Rep*, 2002, 57(9): 26–30.
- [6] TROIVE L, FURUBERG J, SKOGLUND P, ALLROTH S. High density PM components by high velocity compaction, a comparison with conventional compaction [C]//Euro PM 2005. Prague, Czech Republic, Shrewsbury, UK: European Powder Metallurgy Association, 2005.
- [7] WANG Jian-zhong, QU Xuan-hui, YIN Hai-qing, ZHOU Sheng-yu, YI Ming-jun. High velocity compaction of electrolytic copper powder [J]. *The Chinese Journal of Nonferrous Metals*, 2008, 18(8): 1498–1503. (in Chinese)
- [8] CHEN Jin, XIAO Zhi-yu, LI Chao-jie, TANG Cui-yong, XU Yang, ZHANG Fu-bing. High velocity re-striking forming of iron powder [J]. *Powder Metall Industry*, 2010, 20(6): 18–21. (in Chinese)
- [9] SOURIOU D, GOEURIOU P, BONNEFOY O, THOMAS G, DORE F. Influence of the formulation of an alumina powder on compaction [J]. *Powder Technol*, 2009, 190(1–2): 152–159.
- [10] JAUFFRES D, LAME O, VIGIER G, DORE F. Microstructural origin of physical and mechanical properties of ultra high molecular weight polyethylene processed by high velocity compaction [J]. *Polymer*, 2007, 48(21): 6374–6383.
- [11] BARENDVANDEN B, CHRISTER F, TOMAS L. Industrial implementation of high velocity compaction for improved properties [J]. *Powder Metall*, 2006, 49(2): 107–109.
- [12] YAN Z Q, CHEN F, CAI Y X. High-velocity compaction of titanium powder and process characterization [J]. *Powder Technol*, 2011, 208(3): 596–599.
- [13] YAN Zhi-qiao, CHEN Feng, CAI Yi-xiang, CUI Liang. High velocity compaction and characteristics of Ti powder [J]. *Acta Metall Sinica*, 2010, 46(2): 227–232. (in Chinese)
- [14] ERIKSSON M, ANDERSSON M, ADOLFSSON E, CARLSTROM E. Titanium hydroxyapatite composite biomaterial for dental implants [J]. *Powder Metall*, 2006, 49(1): 70–77.
- [15] YAUN B G, LI C F, YU H P, SUN D L. Influence of hydrogen content on tensile and compressive properties of Ti–6Al–4V alloy at room temperature [J]. *Mater Sci Eng A*, 2010, 527(16–17): 4185–4190.
- [16] ABKOWITZ S, ABKOWITZ S M, FISHER H, SCHWARTZ P J. CermeTi® discontinuously reinforced Ti-matrix composites: Manufacturing, properties, and applications [J]. *JOM*, 2004, 56(5): 37–41.
- [17] FERRI O M, EBEL T, BORMANN R. Influence of surface quality and porosity on fatigue behaviour of Ti–6Al–4V components processed by MIM [J]. *Mater Sci Eng A*, 2010, 527(7–8): 1800–1805.
- [18] OBASI G C, FERRI O M, EBEL T, BORMANN R. Influence of processing parameters on mechanical properties of Ti–6Al–4V alloy fabricated by MIM [J]. *Mater Sci Eng A*, 2010, 527(16–17): 3929–3935.

# 粉末粒径对高速压制 Ti–6Al–4V 合金性能的影响

闫志巧<sup>1,2</sup>, 陈峰<sup>1</sup>, 蔡一湘<sup>1</sup>, 尹健<sup>2</sup>

1. 广州有色金属研究院 粉末冶金研究所, 广州 510650;

2. 中南大学 粉末冶金国家重点实验室, 长沙 410083

**摘要:** 采用高速压制(HVC)技术成形平均粒径分别为 103、66 和 44  $\mu\text{m}$  的 3 种 Ti–6Al–4V 合金粉末, 然后将合金粉末进行真空烧结, 考察粉末粒径对成形效果和烧结体性能的影响。结果表明, 细粉末比粗粉末更难压制, 获得的压坯密度也更低。但是细粉末压坯的烧结密度明显高于粗粉末压坯的烧结密度。与粒径为 103 和 66  $\mu\text{m}$  的粉末相比, 粒径为 44  $\mu\text{m}$  的粉末的压坯密度最低, 在冲击能量为 913 J 时其相对密度为 85.1%。然而在 1300  $^{\circ}\text{C}$  烧结 2.5 h 后, 粒径为 44  $\mu\text{m}$  的粉末压坯的烧结密度最高, 其相对密度达到 98.2%。而且, 粒径为 44  $\mu\text{m}$  的烧结试样具有最高的硬度和压缩强度, 分别为 HV 354 和 1265 MPa。

**关键词:** Ti–6Al–4V; 高速压制(HVC); 压坯密度; 烧结

(Edited by Xiang-qun LI)